The Effelsberg–Bonn H I Survey

Test observations with the new 7-Beam receiver

B. Winkel, J. Kerp and P.M.W. Kalberla

December 12, 2007

1 System quality

To evaluate the current status of the new 7-Beam 21-cm receiving system test measurements were performed on November, 20/21 (hereafter referred to as tm1) and November, 23/24, 2007 (tm2). Three FPGA spectrometers were used in parallel, one narrow band unit (1024 spectral channels, 50 MHz) for the detection of the emission of the Milky Way (B1; Stanko et al. 2005), a broad band (8k/16k, 100 MHz) unit originally developed for the APEX telescope covering the whole frequency band of the receiver (B2; Hochgürtel et al. 2007; Klein et al. 2006), and a 16k channel spectrometer already implemented at the 100-m telescope which was used at 100 MHz (B3; Klein et al. 2005). This setup (i.e., B1 and B2) is equivalent to the one which will be used during the proposed Effelsberg survey.

Due to the limited number of backends, feeds could be tested only consecutively. In total 14 channels are available. All measurements were carried out in frequency switching mode (inband) leading to four measurement phases ph1 to ph4 (ph1: sig+cal, ph2: ref, ph3: sig, ph4: ref+cal).

Figure 1 shows in example several snapshot spectra of the calibration source S7 for the central horn and one of the outer horns as observed during tm1 with B1 (upper panels) and B2 (lower panels), respectively. The data were not calibrated with respect to bandpass profile and intensity. In fact, a bandpass calibration using a standard frequency switching scheme (so-called *folding*) is not possible because it can only correct for the intermediate frequency (IF) gain curve. Here, most spectral features (i.e., the bandpass curve) follow the frequency switch meaning they are already present before mixing the high frequency (HF) signal to IF. This effect is clearly visible in the upper left panel showing the central feed, but is also present in the outer horn channels (e.g., lower right panel). Unfortunately, these signals entering the frontend (origin at the moment unknown) introduce a very complex gain curve, making it almost impossible to calibrate the bandpass by other means, e.g., using polynomial fits (baselining). Note, that the lower panels show spectra recorded with different local oscillator (LO) settings.

Another prominent feature is a feed resonance line (Keller, priv. com.) producing a strong broad Gaussian-like signal (right edge of the bandpass for B1 and left edge for B2). The insets in the lower row show the emission line of the source of interest, S7 (left panel), and a very prominent RFI signal caused by terrestrial digital radio (DAB) at a frequency of 1450 MHz. The latter is far outside the bandpass filter but still detectable, showing that the stopband suppression of the frontend filters is not sufficient. In fact, some of the temporal variations of the baseline of the central feed (see below) can be attributed to the very intense linear polarized interference signal of the DAB.

The subsequent paragraphs compile a more quantitative analysis of the receiver.

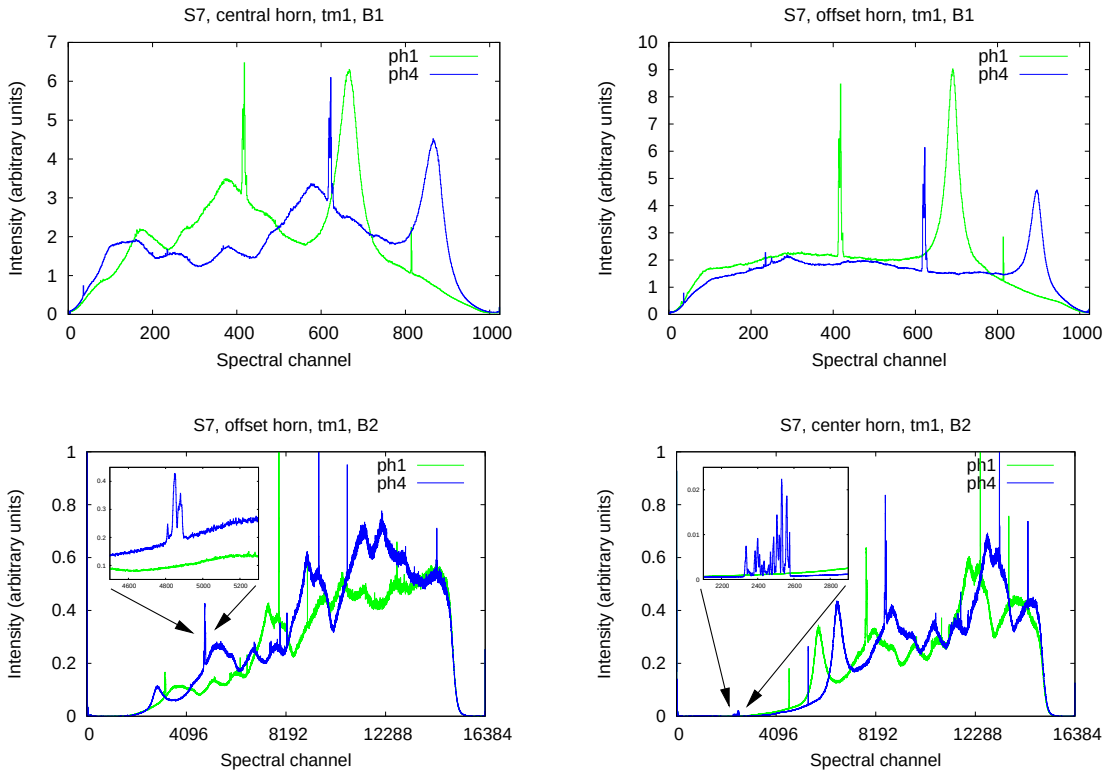

Fig. 1: Uncalibrated S7 spectra as measured during tm1. **Upper left:** Scan 6698, B1, ch1, central feed. Most of the spectral features, i.e., the bandpass shape follow the frequency switch. This makes a bandpass calibration using a standard frequency switching scheme impossible. **Upper right:** Scan 6699, B1, ch1, offset feed. **Lower left:** Scan 6699, B2, ch1, offset feed. The inset shows the signal of interest, the calibration source S7. **Lower right:** Scan 6690, B2, ch1, central feed. The inset shows a very prominent RFI signal located beyond the stopband of the filters which hence should not be detectable. It is caused by terrestrial digital radio (DAB) at a frequency of 1450 MHz.

2 Receiver stability

The stability and sensitivity of the receiver was of highest interest. To evaluate this quantitatively, the so–called *Allan*–plots can be used. A qualitative analysis is also feasible, using greyplots to visualize the dependence of the bandpass shape and gain of time.

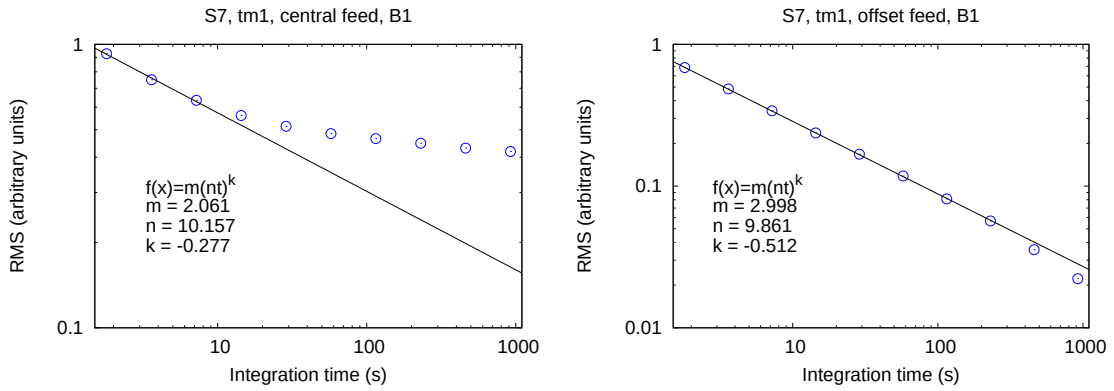

Fig. 2: Allan plot derived from spectra of the calibration source S7, measured during tm2. The left plot shows the noise behaviour of the central feed (scan 6698, tm1, B1, spectral channels 450 to 550) for 512 dumps of 0.45 s integration time each (separated by 2 s). To handle the complex shape of the gain curve a mean spectrum was computed and each individual spectrum was divided by this mean spectrum prior calculating the Allan plot values. The right panel shows the Allan–plot of one of the offset feeds (scan 6699). While the central feed diverges from the theoretical behaviour even after $t_\mathrm{A} \sim 10$ s the offset feed reveals a very good stability/sensitivity up to the maximum measured integration time of about 1000 s.

2.1 *Allan*–plots

For receiving systems in astronomy it is very important that the noise of the system decreases with the square–root of the integration time. For an ideal radio receiver the radiometer equation

$$P(t) \sim \frac{1}{\sqrt{t \cdot \Delta f}} \sim t^{-0.5} \tag{1}$$

is applicable, stating that the noise power $P(t)$ decreases with the square–root of the integration time t and bandwidth Δf. Practically, each system suffers from instabilities on a certain time scale t_A, yielding a divergence from the theoretical behaviour. It is obvious, that a system should be designed in a way to maximize t_A. One possibility to measure the stability is to compute a so–called *Allan*-plot. Several hundred or thousands of short (in time) spectra or "spectral dumps" are recorded and subsequently integrated (e.g., in steps of 2^n) to evaluate the noise on the time scale t_n. The noise level can be measured in various ways: simply compute the RMS for the time series in a given spectral channel, or calculate the baseline RMS using polynomial fits, etc. Due to the complex bandpass shape, we calculate first a mean spectrum and divide each individual spectral dump by this mean spectrum. Accordingly the baseline RMS is then directly given by the standard deviation within a certain spectral range. Note, that this procedure does not have any affect on the

noise properties of the data. The mean spectrum can be treated as an arbitrary constant[1].

In Fig. 2 *Allan*–plots for the the central feed (left panel) and one of the offset feeds (right panel) are computed. The total sample consists of about 900 spectra (0.45 s dump time, recorded every 2 s due to the measurement with four phases) which are used to calculate a mean spectrum. For the actual Allan–plot only 512 of them are used. The central feed has a noise property incompatible with the radiometer equation Eq. (1), with $t_\mathrm{A} \sim 10\,\mathrm{s}$. On the other hand the offset feed even after integration of about 1000 s follows the expected behaviour.

2.2 Bandpass instabilities

The reason for the short Allan–time t_A of the central feed (circular polarization) is a very instable gain curve probably caused by the DAB interference (linearly polarized) signal pumping power into the system. The offset horns are much less sensitive as they measure linear polarization only. The instability can be visualized by using grey–plots, showing the development of the spectra with time; see Fig. 3. Again, a mean spectrum was computed and each spectral dump was divided by it to improve the dynamic range of the grey–plot.

3 System temperature and noise

The measured brightness temperature T_B is usually calculated (in frequency switching mode) by computing

$$T_\mathrm{B} = T_\mathrm{sys}\frac{S_\mathrm{sig} - S_\mathrm{ref}}{S_\mathrm{ref}} = T_\mathrm{sys}\frac{S_\mathrm{sig,cal} - S_\mathrm{ref,cal}}{S_\mathrm{ref,cal}} \tag{2}$$

where T_sys denotes the system temperature of the receiver and S are the measured fluxes (in arbitrary units) during the four frequency switching phases. As T_sys is initially unknown, one needs an indirect tool to convert the spectra to brightness temperatures. One possibility is to use the signal of the noise diode. This might be very errorprone if the noise diode has a non–flat power spectrum itself, is not stable enough, or is simply inaccurate. Therefore, for an absolute calibration one commonly uses a calibration source with a well–known flux. At the 100–m telescope two sources are often used, S7 and S8, respectively.

Unfortunatelly, the bandpass calibration is not applicable in our case (as the overall bandpass shape is influenced too much by the frontend, see Section 2). Hence, we use polynomial fitting (excluding the spectral line region) to estimate the bandpass

[1] The only drawback is, that the RMS values referring to the longest integration times are slightly underestimated. This bias is produced if the overall data–set, for which the mean spectrum was calculated, is not much larger than the sample which was used to calculate the Allan plot.

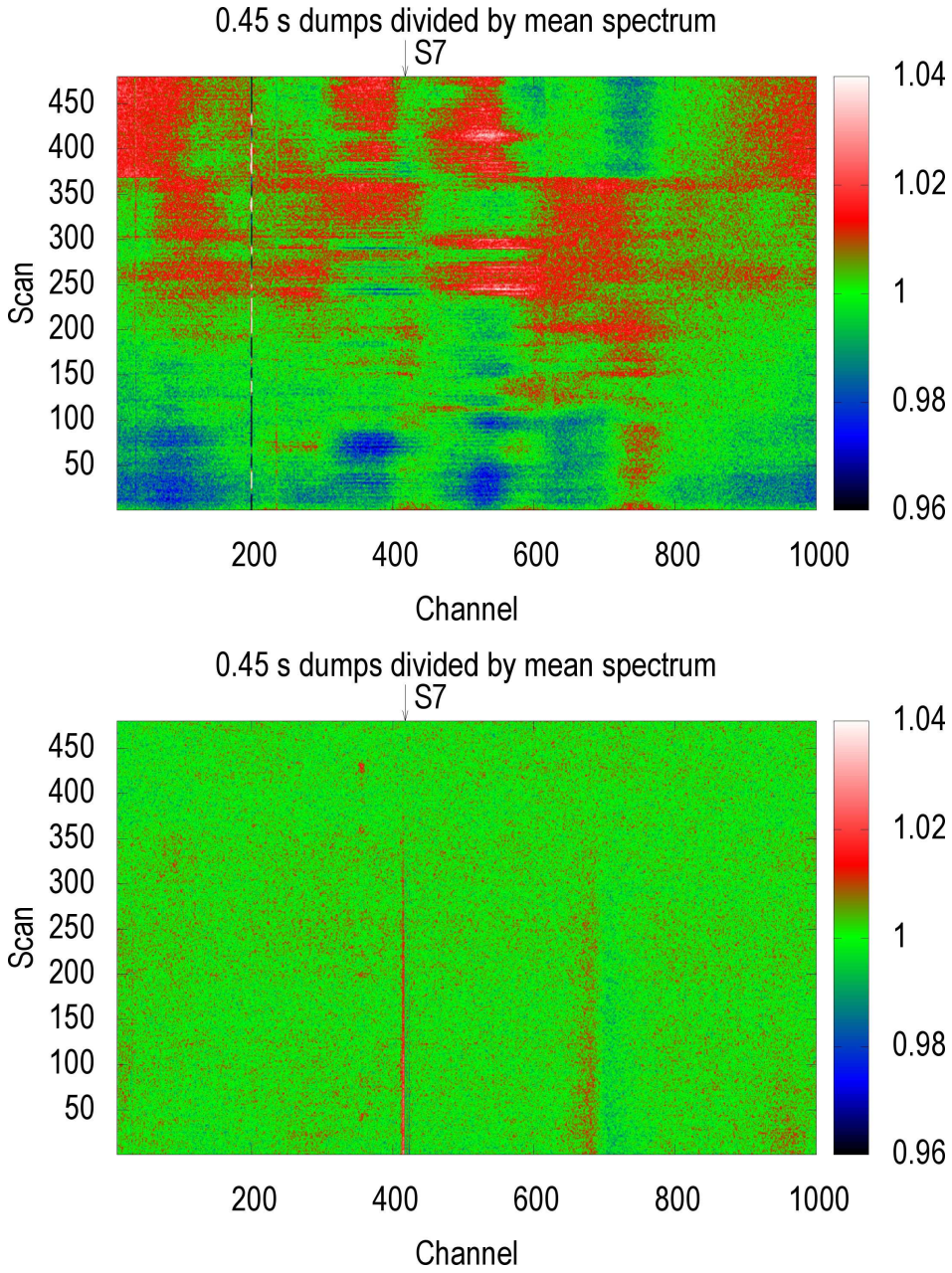

Fig. 3: Testing the temporal bandpass stability of the central feed and one of the offset feeds. The spectral dumps towards the calibration source S7 we plottet time–vs–spectral channels. These greyplots were calculated for the (tm1, B1, Scan 6698/6899, ch1, ph1) with the central (top panel) and one of the offset horns (bottom panel). Because the overall bandpass curves of both feeds are complex each individual dump was divided by a mean spectrum. The top panel reveals time– and frequency–dependend residuals showing the instability of the central feed. The offset horn does not have this problem.

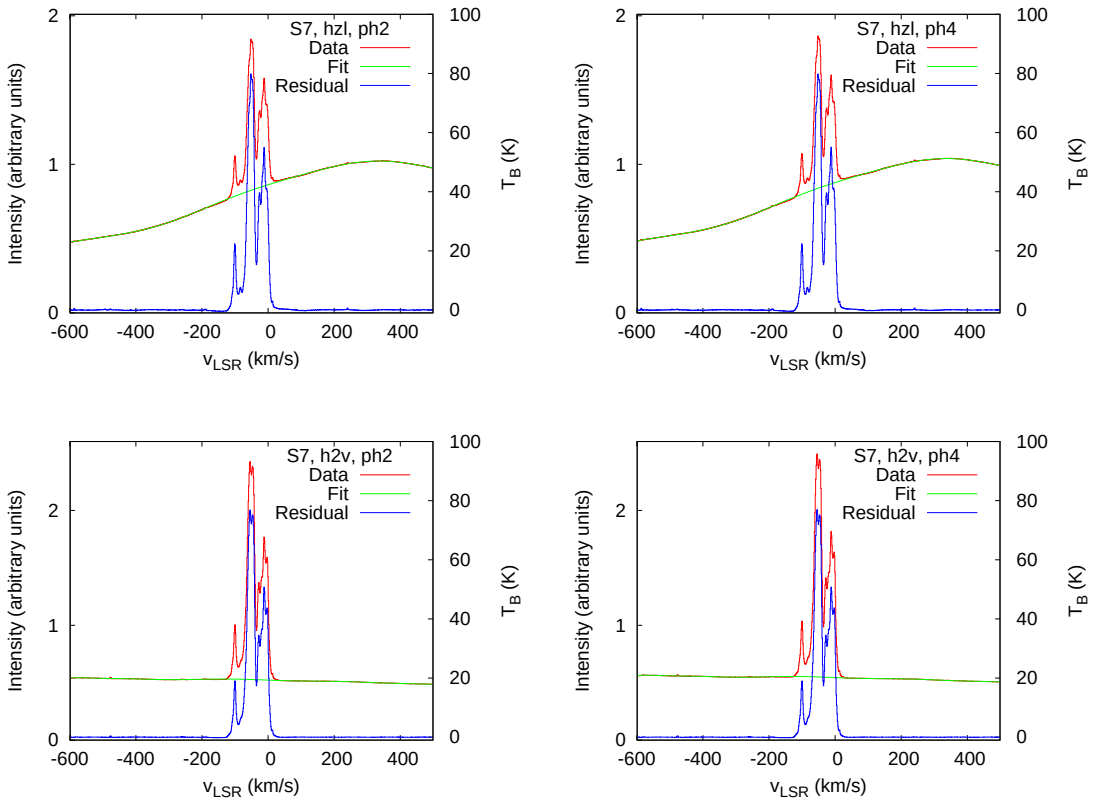

Fig. 4: Calibrated S7 spectra obtained with the central feed measured during tm2. The upper row figures shows the left–hand circular polarization channel of the central feed, the lower row figures feed display the right–hand polarisation channels of the central feed (tm2, B3, Scan 6813) after 650 s of integration. The left panels contain data from ph2, the right panels contain ph4. A polynomial fit (green line) was applied to the raw (uncalibrated) data (red line). The calibrated spectrum was calculated (blue line) as described in the text.

shape. In Eq. (2) we have to substitute the reference signal with the result of our fit. Then a correction factor α can be computed which yields the integrated flux.

Of further interest is the baseline noise (RMS). It is determined from the residual (calibrated) spectrum by computing the standard deviation of a spectral portion of the baseline. Practically, this is not easy to fulfill, as often RFI signals degrade the spectra. Furthermore, the bandpass shape might hardly be described by a low–order polynomial. In fact, both problems make our measurement of the baseline noise very errorprone.

Figures 4 and 5 show calibrated S7 spectra (tm2, B3) for the central feed (left circular, hzl) and three of the offset feeds (2-4, vertical, h2v, h3v, h4v) each for two phases (ph2, ph4). The integration times, as well as, the measured system and noise temperatures are given in Table 1. Each of the panels contains the (uncalibrated)

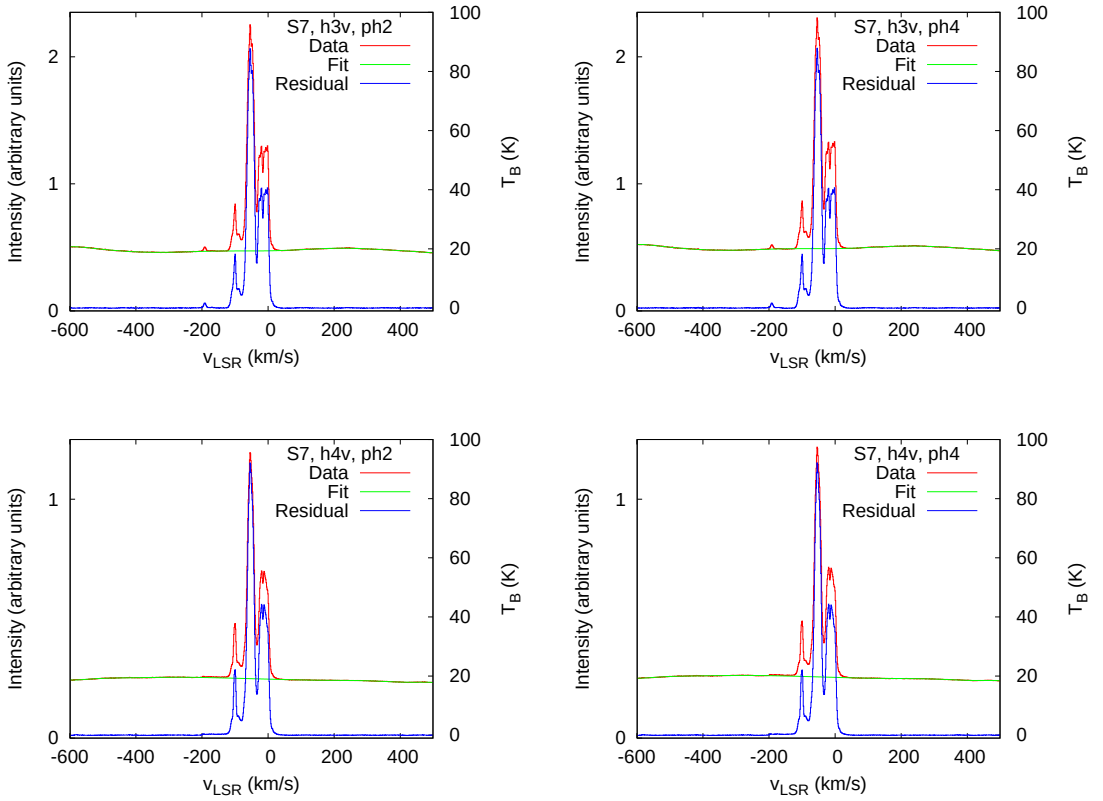

Fig. 5: Calibrated S7 spectra as obtained with an offset feed measured during tm2. The upper row shows the vertical polarization channel of the feed three, the lower row shows feed four vertical (tm2, B3, Scan 6814) after 150 s integration. The left panels contain data from ph2, the right panels contain ph4. A polynomial fit (green line) was applied to the raw (uncalibrated) data (red line). The calibrated spectrum was calculated (blue line) as described in the text.

raw spectra (red line) and the polynomial fit (green line) as well as the calibrated spectrum (in terms of brightness temperature T_B).

As expected, the central feed reveals a very high system temperature $T_\mathrm{sys} \sim 65\,\mathrm{K}$ which is a direct consequence of the bandpass instabilities discussed in Section 2. The offset feeds have much lower system temperatures between $\sim 20 \ldots 25\,\mathrm{K}$. The RMS noise values are good and in the expected range, but show large scatter due to the complicated bandpass shape and probably residual RFI contamination (it is not easy to distinct both). Both features might not be well approximated by the polynomial fit leading to increased RMS values. However, the properties of the receiver – especially for the offset feeds – are very promising.

Table 1: System temperatures and RMS–noise of the calibrated S7 spectra. The noise temperatures are the RMS values converted to a spectral resolution of 1 km/s. RMS was measure two times, left and right of the spectral line. Depending on the specific bandpass shape and possibly RFI signals the values have a scatter of up to 100%. Nevertheless, the system temperature $T_{\rm sys}$ is estimated to better accuracy, as the determination is less affected by the quality of the baseline fit. The central horn has a much higher system temperature – a direct consequence of the bandpass instabilities discussed in Section 2. For the outer horns $T_{\rm sys}$ has good values which are lower than for the old 18/21-cm receiver at Effelsberg.

Horn	Phase	$\tau_{\rm int}$ (s)	$T_{\rm rms1}$ (mK)	$T_{\rm rms2}$ (mK)	$T_{\rm sys}$ (K)
z	2	650	92	131	64.7
z	4	650	93	128	65.3
2	2	650	61	22	21.4
2	4	650	61	23	21.8
3	2	150	56	57	23.3
3	4	150	50	57	23.7
4	2	150	55	37	24.2
4	4	150	57	37	24.6

References

Hochgürtel, S., Bertoldi, F., & Klein, B. 2007, in prep.

Klein, B., Krämer, I., & Wielebinski, R. 2005, URSI General Assembly

Klein, B., Philipp, S. D., Krämer, I., Kasemann, C., Güsten, R., & Menten, K. M. 2006, A&A, 454, L29

Stanko, S., Klein, B., & Kerp, J. 2005, A&A, 436, 391